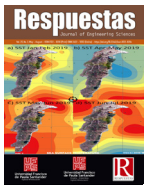

Respuestas
Journal of Engineering Sciences
RESPUESTAS

Original Article https://doi.org/10.22463/0122820X.2189

Mechanical characterization of additive manufacturing composite parts

Caracterización mecánica de materiales compuestos de fabricación aditiva

Juan Sebastian León-Becerra[1*], Octavio A. González-Estrada[2], William Pinto-Hernández[3]

[1*] *PhD. en Ingeniería mecánica, Juan.leon2@correo.uis.edu.co, Orcid: 0000-0002-1740-3127, Universidad Industrial de Santander, Bucaramanga, Colombia.*

[2] *PhD. Mechanical and Materials Engineering, agonzale@uis.edu.co, Orcid: 0000-0002-2778-3389, Universidad Industrial de Santander, Bucaramanga, Colombia.*

[3] *Doutor em Ciências da Engenharia Mecânica, wpintoh@uis.edu.co, Orcid: 0000-0003-0126-6372, Universidad Industrial de Santander, Bucaramanga, Colombia.*

How to cite: J.S. Leon, O.A. González-Estrada, W. Pinto, "Mechanical characterization of additive manufacturing composite parts". *Respuestas,* vol. 25, no. 2, pp. 109-116, 2020.

Received on February 07, 2020; Approved on April 5, 2020

Keywords:

Composite materials, Additive manufacturing, Fusion deposition modeling, Mechanical characterization.

ABSTRACT

Additive Manufacturing is a novel manufacturing method in which the part is produced layer by layer from a 3D CAD model. In this work, we present the mechanical characterization of Fusion Deposition Modeling (FDM). Composite parts made by a nylon matrix with two kinds of fiber reinforcements: carbon fiber or fiberglass. From the obtained microstructure, we perform a division of the composite part in regions, and individual stiffness matrices are encountered by either using a linear elastic isotropic model, for the case of solid matrix filling, or an orthotropic linear elastic model based on micromechanical results. Then, a volume average stiffness method is employed to perform the characterization of the whole part. The theoretical results are compared with the experimental data, showing good agreement for both cases. This research allows the prediction of the structural behavior of additive manufacturing 2composite parts.

Palabras clave:

Materiales compuestos, Manufactura aditiva, Moldeo por deposición fundida, Caracterización mecánica.

RESUMEN

La manufactura aditiva es un método de fabricación reciente en el que la pieza se produce capa por capa a partir de un modelo CAD 3D. En este trabajo, presentamos la caracterización mecánica del Fusion Deposition Modeling (FDM) aplicada a partes compuestas hechas por una matriz de nailon con dos tipos de refuerzos de fibra: fibra de carbono o fibra de vidrio. A partir de la microestructura obtenida, se realiza una división de la parte compuesta en regiones, y se encuentran matrices de rigidez individuales utilizando un modelo isotrópico elástico lineal, para el caso de relleno de matriz sólida, o un modelo elástico ortotrópico lineal basado en resultados micromecánicos. Luego, se emplea un método de rigidez promedio de volumen para realizar la caracterización de la parte completa. Los resultados teóricos se comparan con los datos experimentales, mostrando una buena concordancia en ambos casos. Esta investigación permite la predicción del comportamiento estructural de las piezas compuestas de fabricación aditiva.

Introduction

Additive fabrication is a manufacturing method in which the part is produced layer by layer from a 3D CAD model. Different technologies of additive manufacturing have appeared in recent years [1], [2]. Fusion deposition modeling is an additive manufacturing technology in which a high-temperature extruder is fusing a filament and then deposit onto a bed [3].

Some variations of FDM can produce multi-material extrusion by using double extrusion or co-extrusion methods [4]. Figure 1 shows the Markforged MarkTwo FDM based composite 3D printer used for this research [5]. These methods allow different materials to be employed. However, composite materials are difficult to manufacture this way because of the two or more distinct materials used, orientations, and param .

*Corresponding author.
E-mail Address: Juan.leon2@correo.uis.edu.co (Juan S. Leon)

Figure 1. 3D printer Marforged MarkTwo ®

Udupa *et al*. [6] present an Additive manufacturing (AM) process for the printing of functionally graded materials composed of two different metal phases. AM technologies have also produced reinforced polymers. Dickson *et al*. [7] [8] developed an FDM printing machine that allows the printing of fibers in plain trajectories and with woven architecture. Markforged company [5] was amongst the first ones to produce polymer reinforced composites by additive manufacturing. Some applications of fiber-reinforced polymer composites include grips, robotic arms, and others [9].

Justo *et al*. [10], and many others [11], have performed the experimental characterization of 3D printed composite parts in tension, compression, and in-plane shear test. Pertuz *et al*. [12], [13] evaluated static and dynamic mechanical response for AM composites. Melenka *et al*. [14] use the Volume Average Stiffness (VAS) method, for a composite with Kevlar reinforcement. However, a simplified model [15] is used for the characterization of infill patterns, assuming them as a regular solid infill with a high level of porosity.

Besides support structures, lattices can be used in the infill to reduce the weight of the part by making it more porous. This feature can be useful, for instance, in the hip-joint replacement [16], and in some parts, represent a high volume portion.

In this work, we present the mechanical characterization of AM composite parts produced by the Markforged Mark Two printer, first the characterization of the composite parts is presented, making attention on infill patterns, taking into consideration geometrical characteristics, such as infill density, length of the side as a function of the nozzle diameter, layer thickness and others. Models for finding the specific stiffness of the infill patterns are those presented in [17]. This work presents an improvement by taking into consideration the specific infill architecture characterization. After, a VAS method characterizes the composites and their stiffness matrices. Finally, results compare with experimental data.

Geometrical and mechanical characterization of the composed regions

Typically, an FDM composite part is formed by adding layers of a matrix in both the bottom and the top (called floor and ceiling, which can be solid or as an infill pattern made by a lattice structure. In the middle layers, fiber-reinforced is placed, which can locate in the whole width or just a section of it. Figure 2 shows the most generic transverse section.

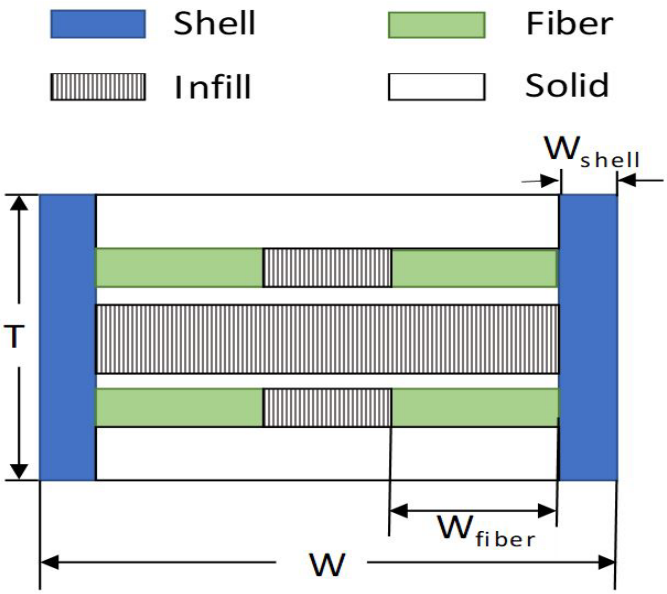

Figure 2. Cross-sectional schematic view

This technology is a 2.5D, which means that fiber can be placed only in the printing plane. Support material serves to create structures such as holes, steep inclined planes, and others, and they allow placement of the last layers. Support material needs remotion afterward. Therefore, lattice structures are great candidates for support material. Lattice are structures that have voids and repeat themselves along a direction.

There are plenty of lattice structures. Common ones are rectangular pattern, triangular or honeycomb. Other

more sophisticated includes gyroids [18], which are the structure that maximizes the surfaces in an allowed volume while maintaining structural integrity. Practically all lattice patterns can be used for infill, however, Markforged 3D printer works with three infill patterns, namely: rectangular, triangular, and honeycomb, which are used in this study.

The infill density refers to the ratio of the volume occupied by the printed material. Table 1 shows the minimum, maximum, and default values of the three most available infill patterns in the Markforged 3D printer: rectangular, triangular, and hexagonal or honeycomb [19].

Table 1. Infill density range

Pattern	Minimum	Maximum	Default Value
Triangular	28%	55%	44%
Rectangular	>0%	92%	50%
Hexagonal	18%	62%	37%

Figure 3 shows the representative unit cell (RUC) with three different infill density for the most common patterns. RUC is the smallest structure that repeats itself along the lattice region.

Figure 3. Different RUC of infill patterns with three infill density following the values presented in Table 1.

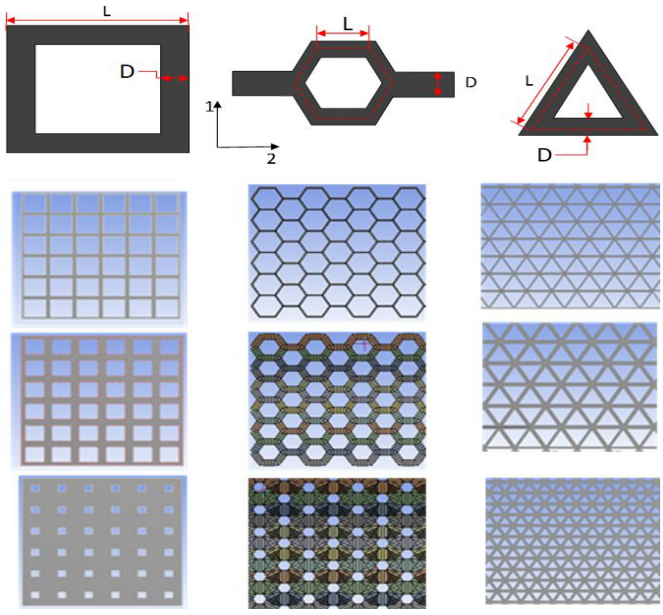

In the next section, we present the Equations used for the mechanical characterization of the different regions.

Honeycomb or hexagonal

Honeycomb pattern use is mostly for compression applications, widely used as a sandwich core in the manufacturing of composite panels. It has excellent strength with fast printing times. The geometrical characterization can be found in Gibson [17], the equations for characterizing it are presented here:

$$E_1 = 2.3E_s(t/l)^3 \quad (1)$$

$$E_2 = E_1 \quad (2)$$

$$G_{12} = 0.57(t/l)^3 \quad (3)$$

$$v_{12} = \frac{(cos\,\theta)^2}{sin\,\theta\,\left(\frac{h}{l}+sin\,\theta\right)} \quad (4)$$

Where t, l and θ refer to the thickness, the length, and the hexagonal angle, respectively. Es represents the elastic modulus of the solid, E_1 the elastic modulus in the preferent fiber direction, E_2 the in-plane elastic modulus transverse to the fiber direction. G_{ij} is the shear elastic modulus, and v_{ij} the Poisson ratio in the ij directions. The density is found through equation (5)

$$Density = \frac{\frac{t}{l}\left(\frac{h}{l}+2\right)}{2cos\,\theta\,\left(\frac{h}{l}+sin\,\theta\right)}, \quad (5)$$

where h is the height of the individual cell.

Rectangular or grid

Rectangular is the standard infill pattern of most of FDM 3D printers. It represents the right balance between strength in all directions and printing time. The representative unit cell (RUC) of the square pattern is a square with side a.

If a constant thickness is assumed, the infill density expresses the ratio of filled area to the total area, for the square pattern, it is given by:

$$Density = \frac{L^2 - (L-2D)^2}{L^2} = \frac{-4D^2L + 2DL}{L^2} \quad (6)$$

Where L and D stand for the side and diameter of the nozzle, respectively. With a 0.1 mm nozzle diameter as a lower bound of D. For this case, we have:

$$E_1 = E_s(t/l) \quad (7)$$
$$E_2 = E_1 \quad (8)$$

Triangular

The triangular infill pattern has high strength along the direction of the wall, so it is more robust than a rectangular pattern but takes more time to print. The triangle pattern is stiffer than the rectangular, as can be inferred from equations 9 and 10

$$E_1 = 1.15E_s(t/l) \quad (9)$$
$$E_2 = E_1 \quad (10)$$

The expression for the density can is given in [17]

Solid and shell regions

For those regions, the model employed was proposed by Rodriguez [15], here reproduced:

$$E_1 = (1-p_1)E_s \quad (11)$$
$$E_2 = (1-\sqrt{p_1})E_s \quad (12)$$
$$E_3 = E_2 \quad (13)$$
$$G_{12} = G\frac{(1-p_1)(1-\sqrt{p_1})}{(1-p_1)+(1-\sqrt{p_1})} \quad (14)$$
$$G_{23} = (1-\sqrt{p_1})G \quad (15)$$
$$v_{12} = v_{13} = (1-p_1)v \quad (16)$$
$$v_{23} = (1-\sqrt{p_1})v \quad (17)$$

where p_1 stands for the porosity value.

Fiber-reinforced region

The mechanical characterization of the fiber-reinforced region is obtained from analytical and semi-analytical expressions [20] of the micromechanical model. Particularly, E_1 and v_{12} are obtained using the Reuss model (rule of mixtures), Voigt model (inverse rule of mixtures) is used for characterizing transverse modulus E_2, cylindrical assemblage for G_{12}, and semi-empirical stress partitioning parameter for G_{23}.

Performing Volume Average Stiffness (VAS) method

The VAS model obtains the overall mechanical response of the part. It consists first in determining each constituent volume and their corresponding volumetric fraction using equations (18-21). Table 2 depicts the nomenclature used for describing the cross-sectional view and gives the values used for the experimental characterization.

Table 2. Nomenclature and used values.

Name	Symbol	Value
Height	H	258 mm
Width	W	12.7 mm
Thickness	T	2.5 mm
Layer Thickness	T_{layer}	0.1 mm
Number of floor layers	N_{floor}	
Shell Width	W_{shell}	mm
Volume	V	mm^3
Volumetric fraction	V_f	dimensionless

The calculation of the volumes depends on the geometrical and process parameters described in Table 2.

$$V_{tensile} = HWT \quad (18)$$
$$V_{floor} = [W - (2W_{shell})]HT_{layer}N_{floor} \quad (19)$$
$$V_{fiber} = W_{fiber}HT_{layer}N_{concentric}2N_{fiber} \quad (20)$$
$$V_{infillfiber} = W_{infillfiber}T_{layer}HN_{fiber}$$
$$\text{With, } W_{infillfiber} = [W - (2W_{shell}) - (W_{fiber}2N_{concentric})] \quad (21)$$

Ceiling, infill, and solid volumes are found by the same equation (19) but replacing the number of layers for the corresponding region. The volumetric fractions V_fi are obtained using equation (22).

$$V_{fi} = \frac{V_i}{V_{tensile}} \quad (22)$$

In which regions of infill, shell, fiber, solid, floor, or ceiling replaces the subscript i.

The next step is to obtain the stiffness matrix of the individual regions. For the solid and shell regions, it is given by the generalized Hooke′s law in a linear elastic solid, the model gives an orthotropic solid, which stiffness matrix S is then given by equation (23).

$$S = \begin{bmatrix} \frac{1}{E_1} & -\frac{\nu_{21}}{E_2} & -\frac{\nu_{31}}{E_3} & 0 & 0 & 0 \\ -\frac{\nu_{12}}{E_1} & \frac{1}{E_2} & -\frac{\nu_{32}}{E_2} & 0 & 0 & 0 \\ -\frac{\nu_{13}}{E_1} & -\frac{\nu_{23}}{E_2} & \frac{1}{E_3} & 0 & 0 & 0 \\ 0 & 0 & 0 & \frac{1}{G_{23}} & 0 & 0 \\ 0 & 0 & 0 & 0 & \frac{1}{G_{13}} & 0 \\ 0 & 0 & 0 & 0 & 0 & \frac{1}{G_{12}} \end{bmatrix} \quad (23)$$

In this work, the equations present by Gibson [17] were employed with the different infill patterns and, then, characterized to obtain the mechanical properties, notably the compliance and stiffness matrices for different infill density values. Employing infill mechanical behavior could give a better estimate than using the model in Melenka [14].

For the composite section, a micromechanical model was employed. Then, for the different layers layup, the used stiffness model for the composite section was the classical laminate theory (CLT).

Once all the stiffness matrices are found, they must be in the same axis, for that, rotation matrices are used, as depicted in equations (23) and (24).

$$S_{xyz} = [T]^T[S][T] \quad (23)$$

$$[T] = \begin{bmatrix} c^2 & s^2 & 0 & 0 & 0 & 2cs \\ s^2 & c^2 & 0 & 0 & 0 & -2cs \\ 0 & 0 & 1 & 0 & 0 & 0 \\ 0 & 0 & 0 & c & -s & 0 \\ 0 & 0 & 0 & s & c & 0 \\ -cs & cs & 0 & 0 & 0 & c^2 - s^2 \end{bmatrix} \quad (24)$$

Where [T] stands for transformation matrix, s and c for sinus and cosines of the angle. The transformation must be performed because the fibers or the raster may not be aligned with the direction of the applied force.

Finally, all stiffness matrices are summed up by taking into account their corresponding volumetric fractions, as show in equation (25).

$$[C^G] = V_{fshell}[C_{shell}] + V_{finfill}[C_{infill}] + V_{fsolid}[C_{solid}] + V_{ffiber}[C_{fiber}] \quad (25)$$

In order to determine the effective engineering properties, the general stiffness matrix S^G is inverted into the general compliance matrix C^G, and the engineering constants are found as indicated in equations (26) and (27).

$$S^G = [C^G]^{-1} \quad (26)$$

$$\{E_x \quad E_y \quad E_z \quad G_{xy} \quad G_{yz} \quad G_{xz} \quad \nu_{xy} \quad \nu_{zx} \quad \nu_{xy}\} = = \left\{\frac{1}{S_{11}^g} \quad \frac{1}{S_{22}^g} \quad \frac{1}{S_{33}^g} \quad \frac{1}{S_{66}^g} \quad \frac{1}{S_{44}^g} \quad \frac{1}{S_{55}^g} \quad \frac{-S_{12}^g}{S_{11}^g} \quad \frac{-S_{13}^g}{S_{33}^g} \quad \frac{-S_{23}^g}{S_{22}^g}\right\} \quad (27)$$

Numerical values of the model were obtained with an assumed porosity of 10 %, E is the elastic modulus of the nylon at 380 MPa, and 0.30 in Poisson ratio. For the fiber, 72 GPa of elastic modulus and 30% fiber content was used [21].

Results and discussion

We perform a tensile test on MTS Bionix Machine following the ASTM D3039M procedure, to assess the

validity of the model. With a selected speed of 2 mm/min and five samples. Samples are rectangular with a width of 27 mm and 200 mm of length, with a thickness of 2.5 mm. Tabs are located at the ends to ensure a better grip.

The samples were 3D printed from the MarkTwo and are from a Nylon Matrix and fiberglass-reinforced layers, Infill region is taken triangular with a relative density of 37% and four layers (N_{infill}). The solid region accounts for thirteen layers (N_{solid}) with a porosity value p1 of 0.1, and the fiber-reinforced region for the other eight layers at 0° orientation. The materials properties used were E_s 940 MPa and v_s of 0.39 for the nylon, tensile modulus of the fiber was 70 GPa, and the poisons ratio ν 0.22.

Figure 4. Tensile test and fracture

The maximum average force was 13715.2 N, with a displacement of almost 12 mm. Longitudinal modulus was obtained from tensile data, with a value of 6494 MPa, and then, compared with the model here presented, the VAS value found was 6855 MPa, which gives an average error of 5.3%.

The error between the numerical model and experimental data might be explained due to the uncertainty in void porosity of non-reinforced regions, thickness variations in the manufacturing process.

The VAS model accurately retrieves the stiffness matrix and the engineering constants in terms of the volumetric fraction and the mechanical behavior of each material region. It predicts the behavior in a tensile test stress state, however, due to the assumption of constant strain in the section, the VAS does not take into account the order in which the plies are layed-up, meaning that for other load states, such as bending, in which distance from the neutral-axis is a considerable factor, the model could not be applied. Thus, authors recommend using classical approaches for composite materials such as the classical laminate theory or first shear order deformation.

Conclusions

The model predicts quite well the mechanical characterization, which is the stiffness prediction of the composite part. Further work must be done in characterizing different infill architectures as well as different volumetric ratios.

This work presents a modification of the VAS models, which accounts for the infill architecture and density ratio, typically the infill region has a negligible behavior on the stiffness values. However, if the infill volumetric fraction increases, the error committed to considering the infill as a solid model with porosity could be significant.

Further work will look at the validity of Gibson-Ashby coefficients in AM polymers and the applicable range of relative densities for the geometry of the pattern.

References

[1] T. D. Ngo, A. Kashani, G. Imbalzano, K. T. Q. Nguyen, and D. Hui, "Additive manufacturing (3D printing): A review of materials, methods, applications and challenges," *Compos*. Part B Eng., vol. 143, no. December 2017, pp. 172–196, 2018, doi: 10.1016/j.compositesb.2018.02.012.

[2] E. D. Valbuena-Niño, J. L. Endrino-Armenteros, H. A. Estupiñan-Duran, B. Pérez-Gutiérrez, and A. Díaz-Lantada, "Caracterización microscópica de texturas superficiales fabricadas aditivamente mediante estereolitografía láser," *Respuestas*, vol. 21, no. 2, p. 37, Jul. 2016, doi: 10.22463/0122820X.771.

[3] T. Hofstätter, D. B. Pedersen, G. Tosello, and H. N. Hansen, "State-of-the-art of fiber-reinforced polymers in additive manufacturing technologies," *J. Reinf. Plast. Compos*., vol. 36, no. 15, pp. 1061–1073, 2017, doi:

10.1177/0731684417695648.

[4] J. S. León, J. G. Díaz-Rodríguez, and O. A. González-Estrada, "Daño en partes de manufactura aditiva reforzadas por fibras continuas," *Rev. UIS Ing*., vol. 19, no. 2, pp. 161–176, 2020, doi: 10.18273/revuin.v19n2-2020018.

[5] G. Thomas, M. Antoni, and S. Gozdz, "Three dimensional printer with composite filament fabrication." 2015.

[6] G. Udupa, S. S. Rao, and K. V Gangadharan, "Functionally Graded Composite Materials: An Overview," *Procedia Mater*. Sci., vol. 5, pp. 1291–1299, 2014, doi: 10.1016/j.mspro.2014.07.442.

[7] A. N. Dickson, K. A. Ross, and D. P. Dowling, "Additive manufacturing of woven carbon fibre polymer composites," *Compos. Struct*., vol. 206, pp. 637–643, 2018, doi: 10.1016/j.compstruct.2018.08.091.

[8] A. N. Dickson, J. N. Barry, K. A. McDonnell, and D. P. Dowling, "Fabrication of continuous carbon, glass and Kevlar fibre reinforced polymer composites using additive manufacturing," *Addit. Manuf*., vol. 16, pp. 146–152, Aug. 2017, doi: 10.1016/j.addma.2017.06.004.

[9] P. Parandoush and D. Lin, "A review on additive manufacturing of polymer-fiber composites," *Compos. Struct*., vol. 182, pp. 36–53, 2017, doi: 10.1016/j.compstruct.2017.08.088.

[10] J. Justo, L. Távara, L. García-Guzmán, and F. París, "Characterization of 3D printed long fibre reinforced composites," *Compos. Struct.*, vol. 185, no. October 2017, pp. 537–548, 2018, doi: 10.1016/j.compstruct.2017.11.052.

[11] I. Sierra Nossa, O. Bohórquez, A. Pertuz, H. G. Sánchez Acevedo, and O. A. González-Estrada, "Tensile mechanical properties of composite materials with continuous fiber produced by additive manufacturing," *J. Phys. Conf. Ser*., vol. 1386, no. 012008, pp. 1–7, 2019, doi: 10.1088/1742-6596/1386/1/012008.

[12] A. D. Pertuz, S. Díaz-Cardona, and O. A. González-Estrada, "Static and fatigue behaviour of continuous fibre reinforced thermoplastic composites manufactured by fused deposition modelling technique," *Int. J. Fatigue*, vol. 130, p. 105275, 2020, doi: 10.1016/j.ijfatigue.2019.105275.

[13] O. A. González-Estrada, A. D. Pertuz Comas, and J. G. Díaz Rodríguez, "Monotonic load datasets for additively manufactured thermoplastic reinforced composites," *Data Br.,* vol. 29, p. 105295, Apr. 2020, doi: 10.1016/j.dib.2020.105295.

[14] G. W. Melenka, B. K. O. Cheung, J. S. Schofield, M. R. Dawson, and J. P. Carey, "Evaluation and prediction of the tensile properties of continuous fiber-reinforced 3D printed structures," *Compos. Struct*., vol. 153, pp. 866–875, Oct. 2016, doi: 10.1016/j.compstruct.2016.07.018.

[15] J. F. Rodríguez, J. P. Thomas, and J. E. Renaud, "Mechanical behavior of acrylonitrile butadiene styrene fused deposition materials modeling," *Rapid Prototyp. J*., vol. 9, no. 4, pp. 219–230, 2003, doi: 10.1108/13552540310489604.

[16] C. M. B. Ho, S. H. Ng, and Y.-J. Yoon, "A review on 3D printed bioimplants," *Int. J. Precis. Eng. Manuf*., vol. 16, no. 5, pp. 1035–1046, May 2015, doi: 10.1007/s12541-015-0134-x.

[17] L. J. Gibson and M. F. Ashby, *Cellular solids: Structure and properties, second edition*, 2nd ed. Cambridge: Cambridge University Press, 2014.

[18] S. N. Khaderi, V. S. Deshpande, and N. A. Fleck, "The stiffness and strength of the gyroid lattice,"

Int. J. Solids Struct., vol. 51, no. 23–24, pp. 3866–3877, 2014, doi: 10.1016/j.ijsolstr.2014.06.024.

[19] J. D. Arguëllo-Bastos, O. A. González-Estrada, C. A. Ruiz-Florián, A. D. Pertuz-Comas, and E. D. V-Ninõ, "Study of mechanical properties under compression failure in reinforced composite materials produced by additive manufacturing," *J. Phys. Conf. Ser*., vol. 1126, no. 1, 2018, doi: 10.1088/1742-6596/1126/1/012005.

[20] E. J. Barbero, *Finite Element Analysis of Composite Materials Using ANSYS*, 2nd ed. Boca Ratón, Florida: CRC Press, 2013.

[21] L. G. Blok, M. L. Longana, H. Yu, and B. K. S. Woods, "An investigation into 3D printing of fibre reinforced thermoplastic composites," *Addit. Manuf*., vol. 22, pp. 176–186, 2018, doi: 10.1016/j.addma.2018.04.039.